Published in final edited form as:
*Circ Heart Fail*. 2010 March ; 3(2): 294–305. doi:10.1161/CIRCHEARTFAILURE.109.903450.

# Vitamin B1 Analog Benfotiamine Prevents Diabetes-Induced Diastolic Dysfunction and Heart Failure Through Akt/Pim-1–Mediated Survival Pathway

**Rajesh G. Katare, MD**, **Andrea Caporali, PhD**, **Atsuhiko Oikawa, PhD**, **Marco Meloni, PhD**, **Costanza Emanueli, PhD**, and **Paolo Madeddu, MD**
Experimental Cardiovascular Medicine, Bristol Heart Institute, University of Bristol, United Kingdom.

## Abstract

**Background—**The increasing incidence of diabetes mellitus will result in a new epidemic of heart failure unless novel treatments able to halt diabetic cardiomyopathy early in its course are introduced. This study aimed to determine whether the activity of the Akt/Pim-1 signaling pathway is altered at critical stages of diabetic cardiomyopathy and whether supplementation with vitamin B1 analog benfotiamine (BFT) helps to sustain the above prosurvival mechanism, thereby preserving cardiomyocyte viability and function.

**Methods and Results—**Untreated streptozotocin-induced type 1 or leptin-receptor mutant type 2 diabetic mice showed diastolic dysfunction evolving to contractile impairment and cardiac dilatation and failure. BFT (70 $mg/kg^{-1}/d^{-1}$) improved diastolic and systolic function and prevented left ventricular end-diastolic pressure increase and chamber dilatation in both diabetic models. Moreover, BFT improved cardiac perfusion and reduced cardiomyocyte apoptosis and interstitial fibrosis. In hearts of untreated diabetic mice, the expression and activity of Akt/Pim-1 signaling declined along with O-*N*-acetylglucosamine modification of Akt, inhibition of pentose phosphate pathway, activation of oxidative stress, and accumulation of glycation end products. Furthermore, diabetes reduced signal transducer and activator of transcription 3 phosphorylation independently of Akt. BFT inhibited these effects of diabetes mellitus, thereby conferring cardiomyocytes with improved resistance to high glucose-induced damage. The phosphoinositide-3-kinase inhibitor LY294002 and dominant-negative Akt inhibited antiapoptotic action of BFT and Pim-1 upregulation in high glucose-challenged cardiomyocytes.

**Conclusions—**These results show that BFT protects from diabetes mellitus-induced cardiac dysfunction through pleiotropic mechanisms, culminating in the activation of prosurvival signaling pathway. Thus, BFT merits attention for application in clinical practice.

### Keywords

diabetes mellitus; cardiomyopathy; diastolic dysfunction; benfotiamine; apoptosis



Correspondence to Paolo Madeddu, MD, Chair Experimental Cardiovascular Medicine, Bristol Heart Institute, University of Bristol, Level 7, Bristol Royal Infirmary, Upper Maudlin St, Bristol BS28HW, United Kingdom. madeddu@yahoo.com.

The online-only Data Supplement is available at http://circheartfailure.ahajournals.org/cgi/content/full/CIRCHEARTFAILURE.109.903450/DC1.

Disclosures
None.


Europe PMC Funders Author Manuscripts

Diabetes mellitus (DM) is a potent and prevalent risk factor for heart failure independent of coronary artery disease or hypertension.1 Diabetic cardiomyopathy has an insidious onset and remains, therefore, undiagnosed and untreated in a large number of patients. Furthermore, recent studies have shown evidence of diastolic dysfunction in up to 75% of young, asymptomatic patients with type 1 or type 2 DM.2 The association of diastolic dysfunction and microangiopathy synergistically increases the risk of heart failure, thus pointing out the urgent need of early mechanistic treatment.3,4

A variety of molecular alterations have been associated with diabetic cardiomyopathy, including defects in calcium homeostasis5 and substrate metabolism,6 accumulation of advanced glycation end products (AGE),7 activation of the hexosamine pathway,8 and oxidative stress leading to cardiomyocyte apoptosis.9 However, early stage mechanisms remain mostly unknown.

The pivotal role of the phosphoinositide-3-kinase (PI3K)/Akt/proviral integration site for the Moloney murine leukemia virus-1 (Pim-1) signaling pathway in the control of cardiac contractile function and cardiomyocyte growth and survival is well established.10-12 Of note, the hearts of mice with long-standing DM show decreased levels of activated Akt,13 and intriguingly, signal transducer and activator of transcription 3 (STAT3 [an upstream modulator of Pim-1])-deficient mice spontaneously develop a form of dilated cardiomyopathy similar to that occurring in diabetic mice.14 However, to the best of our knowledge, no information exists on whether altered glucose metabolism may dampen the activity of the STAT3/Akt/Pim-1 trio from early phases of cardiomyopathy and whether pharmacological manipulation of such kinases could help to halt DM-induced cardiac damage.

The conversion of glucose to pentose is hampered in DM because of the inhibition of pivotal enzymes of the pentose phosphate pathway, such as transketolase and glucose-6-phosphate dehydrogenase, resulting in depletion of reducing agents and accumulation of glycolysis end products.15,16 Inhibition of transketolase activity was ascribed to deficit of its coenzyme thiamine. This situation is further aggravated by the fact that increased reactive oxygen species induces compensatory activation of the DNA-repairing enzyme poly(ADP-ribose) polymerase, which in turn inhibits the activity of GAPDH, a crucial enzyme of glycolysis. Intermediate metabolites of glycolysis consequently are forced down to alternative pathways, including AGE formation and hexosamine pathway, which are responsible for protein modification and inactivation and cardiovascular damage.17,18

The aim of this study was 2-fold: (1) to verify whether high glucose might alter STAT3/Akt/Pim-1 expression and activity from early stages of cardiomyopathy and (2) to determine whether benfotiamine (BFT) supplementation can sustain prosurvival signaling and prevent cardiac dysfunction in DM. The rationale of BFT supplementation is to correct thiamine deficit and thereby provide a shunt for glucose through the pentose pathway. Results of this study show the chronological alterations in the prosurvival signaling during the progression of diabetic cardiomyopathy and its correction by treatment with BFT.

## Methods

Details are provided in the online-only Data Supplement in Expanded Materials and Methods.

### Ethics

Experiments were performed in accordance with the *Guide for the Care and Use of Laboratory Animals* (the Institute of Laboratory Animal Resources, 1996) and with approval

of the British Home Office and the University of Bristol. Type 1 diabetes was induced in male CD1 mice (Charles River, United Kingdom) by injection of streptozotocin (40 mg/kg body weight IP per day for 5 days).19 Age-matched animals that received streptozotocin vehicle served as nondiabetic (healthy) controls. In addition, male obese leptin-receptor mutant BKS.Cg-+*Lepr*$^{db}$/+*Lepr*$^{db}$/OlaHsd mice (Harlan, United Kingdom) were used as a model of insulin-resistant type 2 DM. Increases of blood glucose begin at 4 to 8 weeks in these mutant mice. Age-matched lean mice (BKS.Cg-m+/+*Lepr*$^{db}$/OlaHsd) were used as control.

### Treatment Protocol

The experimental protocols are summarized in supplemental Figure IA and IB. Type 1 DM mice were randomly assigned to receive BFT (70 mg/kg body weight/day) or vehicle (1 mmol/L HCl) in drinking water starting at 4 weeks from DM induction (last day of streptozotocin injection) throughout the study. Type 2 DM mice were similarly randomized to treatments starting from 9 weeks of age. The elected BFT dosage reportedly produces a 4-fold increase in plasma thiamine.19,20 Gender- and age-matched healthy (for type 1 DM) or db/+ (for type 2 DM) mice of the same genetic background of the diabetic ones were given vehicle or BFT and used as reference.

### Biochemical Measurements

Confirmation of DM was achieved by measurements of blood glucose levels through the study (supplemental Figure II). Transketolase, glucose-6-phosphate dehydrogenase, and GAPDH activities in peripheral blood erythrocytes and left ventricular (LV) tissue were measured at the time of euthanizing as described previously (n=5 mice per group).16,17,21 AGE levels were measured by ELISA (n=5 mice per group).22

### Echocardiography

Dimensional and functional parameters were measured using a high-frequency, high-resolution echocardiography system. LV chamber dimensions, LV ejection fraction, and LV fractional shortening were determined as described previously.23

### Measurement of LV Pressures and Cardiac Dimensions

LV pressure was measured in anesthetized mice (n=10 to 12 per group) before killing, using a high-fidelity 1.4F transducer-tipped catheter.

### Measurement of Blood Flow

Myocardial blood flow was assessed by the use of fluorescent microspheres, which were injected into the LV cavity (n=4 to 6 mice per group).24

### Immunohistochemistry

Immunohistochemical techniques were used to identify myocardial endothelial cells (isolectin B4 staining) and smooth muscle cells ($\alpha$-smooth muscle actin), fibrosis (sirius red), apoptosis (TUNEL), and hydroxyl radicals (8-hydroxydeoxyguanosine). Superoxides were revealed using dihydroethidium staining of LV cryostat sections.

### In Vitro Studies

**Prosurvival Effect of BFT on High Glucose-Challenged Cardiomyocytes—**HL-1 cardiomyocytes (a gift from Prof William Claycomb, Louisiana State University Medical Center, New Orleans, La) were cultured in the presence of high D-glucose (HG, 30 mmol/L) or normal glucose (5 mmol/L) added with 25 mmol/L D-mannitol as osmotic control. After

72 hours, cells were supplemented with either BFT (150 μmol/L) or vehicle (1 mmol/L HCl) for a further 24 hours. Optimal BFT concentration was decided on the basis of pilot titration studies (supplemental Figure IIIA). In addition, a fixed dosage of BFT was tested to contrast the apoptotic effect of increasing doses of D-glucose (supplemental Figure IIIB). At the end of the experiments, cardiomyocytes were collected for measurement of caspase-3/7 activity performed in 6 wells per each condition and repeated 3 times.

### Inhibition of PI3K, Akt, or STAT3

To verify the involvement of PI3K/Akt in BFT-induced prosurvival effects, we used either the PI3K inhibitor LY-294002 (50 μmol/L) or hemagglutinin-tagged dominant negative mutated form of Akt (*Ad.DN-Akt,* K179 mol/L) or control *Ad.Null* (both at 100 multiplicity of infection). 25 In a separate study, HG-treated HL-1 cardiomyocytes were exposed for 30 minutes to STAT3 inhibitor peptide (Ac-PpYLKTK-OH, 1 mmol/L), a cell permeable compound that reduces the levels of active STAT3 and inhibits DNA-binding activity of STAT3 by forming an inactive STAT3-peptide complex.26 This exposure is followed by treatment with BFT or vehicle. After an additional 24 hours, cells were used for caspase-3/7 activity and Western blot analyses as described earlier. Western blot analyses were performed in triplicates and repeated 3 times, and caspase-3/7 activity was performed in 6 wells per each condition and repeated 3 times.

### Expressional Studies

Western blot analyses were performed on LV samples and HL-1 cardiomyocytes to verify the effects of DM, HG, and treatment on total and pSTAT3 (Tyr705), protein phosphatase 2A (PP2A), total and pe-nitric-oxide synthase (Ser1177), total and pAkt (Ser473), Pim-1, total and pBad (Ser112), Bcl-2, total and p-forkhead box O-1 (pFOXO-1), and cleaved caspase-3 expression.

To assess the O-*N*-acetylglucosamine (GlcNAc) modification of Akt, LV extracts were immunoprecipitated with anti-Akt antibody. 27 The precipitate was then immunoblotted with antibodies for O-GlcNAc (1:10 000, a gift from Prof G.W. Hart, Johns Hopkins University School of Medicine, Baltimore, Md)28 and for total and pAkt. Akt activity in protein extracts was measured with a commercial kit.

Quantitative reverse transcription polymerase chain reaction for mouse Pim-1 and 18s rRNA (for normalization) was performed in a LightCycler. All the expressional analyses were performed on 4 biological replicates.

### Statistical Analysis

Results are presented as mean±SD. The hemodynamic and echocardiographic measurements were compared by the use of repeated measures 2-way ANOVA (factorial design, 2 independent variables [treatment and presence or absence of diabetes]), followed by pairwise comparison using the Holm-Sidak method. For the histological, biochemical, and morphometric analyses, differences between multiple groups were analyzed with 1-way ANOVA and differences between 2 groups with *t* test (paired or unpaired as appropriate). For blood flow and molecular expressional studies, when normality test fails, differences between groups were analyzed using Siegel-Tukey test. Survival curves were analyzed by the Kaplan–Meier method, and comparisons were made with the Gehan-Breslow log-rank test using SigmaStat statistical software. A $P<0.05$ is considered statistically significant for all the parameters.

## Results

### BFT Attenuates DM-Induced Cardiac Remodeling and Dysfunction

The murine models used in this study showed distinct phases in the evolution of cardiomyopathy. The initial phase consisted of diastolic dysfunction, as indicated by the significant decrease in Doppler E/A ratio at 4 weeks from type 1 DM induction (Figure 1A). A similar figure was observed in 9-week-old type 2 diabetic mice (Figure 2A). BFT partially rescued the reduced the E/A ratio and prevented the further deterioration of diastolic function with duration of DM in both diabetic models (Figures 1A and 2A, $P<0.01$ versus healthy controls for both comparisons).

The second phase consisted of impaired contractile performance and cardiac dilatation. In type 1 diabetic mice, systolic function started decreasing from 12 weeks of DM, as indicated by the progressive reduction in LV ejection fraction and LV fractional shortening (Figure 1B). The late stage was characterized by LV chamber enlargement, LV wall thinning, and critical fall in cardiac output, which are typical features of heart failure (Figure 1B and supplemental Figure IVA). Analysis of LV pressure indices and pressure-volume loops further verified the marked dysfunction of diabetic hearts (Figure 1C). In type 2 diabetic mice, systolic dysfunction was precocious, being already apparent at 9 weeks of age and rapidly advancing toward heart failure (Figure 2 and supplemental Figure IVB). Importantly, BFT treatment resulted in the global improvement of LV performance, pressure indices, and volumes in both diabetic models (Figures 1 and 2 and supplemental Figure IV, $P<0.01$ versus vehicle-treated diabetic mice for all parameters) but did not affect cardiac function in healthy mice (data not shown). Inotropic and lusitropic responses to adrenergic stimulation were blunted in type 1 diabetic mice ($P<0.01$ versus healthy controls) but improved by BFT ($P<0.01$ versus vehicle-treated diabetic mice, supplemental Figure V).

### BFT Improves Survival Rate

The survival rate for type 1 diabetic mice was less than that for healthy controls but was remarkably improved by BFT (supplemental Figure VI, $P<0.001$ versus vehicle-treated diabetic mice).

### BFT Improves Myocardial Blood Flow

As shown in Figure 3A, myocardial perfusion was reduced by DM, with this defect being prevented by BFT in both diabetic models ($P<0.01$ versus vehicle-treated diabetic mice). Concordantly, capillary density was reduced in the LV of diabetic mice ($P<0.001$ versus healthy controls) and partially conserved by BFT ($P<0.01$ versus vehicle-treated diabetic mice, Figure 3B). Fractional analysis of arteriole density revealed a marked decrease in small (<30 $\mu$m diameter) arterioles in the LV of both diabetic models ($P<0.001$ versus healthy controls for both comparisons), which was inhibited by BFT ($P<0.001$ versus vehicle-treated diabetic mice for both comparisons, Figure 3C).

### Histological Validation of BFT Effects

Cardiomyocyte cross-sectional area was reduced in type 1 diabetic mice (66±8 $\mu m^2$ versus 83±6 $\mu m^2$ in healthy controls; $P<0.01$) and preserved by BFT (79±7 $\mu m^2$; $P<0.01$ versus vehicle-treated diabetic mice). BFT remarkably prevented cardiomyocyte apoptosis and interstitial fibrosis in both diabetic models (Figure 4; $P<0.01$ for both comparisons).

### BFT Activates the Pentose Phosphate Shunt Pathway and Reduces Oxidative Stress

We found that the activity of transketolase, glucose-6-phosphate dehydrogenase, and GAPDH is reduced in diabetic hearts (Figure 5A through 5C) and associated with marked

increase in AGE (Figure 5D) and O-GlcNAc protein modification (see later). BFT prevented these effects and avoided the increase in reactive oxygen species levels in the heart of both diabetic models (Figure 5E and supplemental Figure VII; $P<0.01$ versus vehicle-treated diabetic mice for both comparisons).

### BFT Prevents DM-Induced Downregulation of STAT3/Akt/Pim-1

Surprisingly, at initial stages, type 1 diabetic hearts showed increased pAkt and peNOS levels but low Pim-1 protein (Figure 6) and mRNA expression (supplemental Figure VIIIA). Importantly, Pim-1 continuously decreased with progression of cardiomyopathy in parallel with accruing changes in its upstream modulators. In temporal sequence, the first change consisted of the decrease in the activated form of STAT3 (STAT3-p-Tyr705), which reportedly induces Pim-1 expression.29 This decrease was followed by an increase in PP2A, which is known to induce Pim-1 mRNA downregulation and protein degradation (data not shown).30 At a later stage, when heart failure was overtly manifested, the diabetic myocardium showed reduced pAkt (Figure 6B) and Akt activity (Figure 6J) and increased O-GlcNAc modification of Akt, which was previously associated with Akt inhibition (Figure 6K).31 Levels of peNOS and pFOXO-1 also were decreased in the failing heart of type 1 diabetic mice (Figure 6C and 6D).

Previous studies showed that both Akt and Pim-1 phosphorylates the proapoptotic Bad, resulting in the formation of Bad-(14 to 3-3) protein homodimer, which leaves Bcl-$X_L$ and Bcl-2 free to inhibit apoptosis.11,32,33 We found that down-regulation of Akt/Pim-1 signaling by type 1 DM is associated to reduced pBad (Ser 112) and Bcl-2 levels and increased cleaved caspase-3 (Figure 6G through 6I).

The heart of type 2 diabetic mice exhibited a marked decrease in STAT3/Pim-1 and modification of Pim-1 downstream effectors but at variance with type 1 DM, also showed an early reduction in Akt phosphorylation and activity (Figure 7). The global depression of STAT3/Akt/Pim-1 was mirrored by a more rapid evolution of cardiomyopathy.

Importantly, BFT prevented the downregulation of STAT3 and Pim-1 and the O-GlcNAc modification of Akt, thereby preserving Akt activity and downstream targets in both diabetic models (Figures 6 and 7). In contrast, myocardial PP2A levels remained increased in BFT-treated diabetic mice (data not shown).

Finally, to verify the direct action of BFT on cardiomyocytes, we performed in vitro assays in which adult cardiomyocytes were cultured in HG or normal glucose in the presence of BFT or vehicle. Consistent with in vivo experiments, HG increased cardiomyocyte apoptosis, this effect being prevented by BFT (supplemental Figure IXA). The antiapoptotic action of BFT was paralleled by conservation of Pim-1 at mRNA (supplemental Figure VIIIC) and protein level (supplemental Figure IXB) and inhibition of HG-induced effects on pBad and Bcl-2 (supplemental Figure IXC and IXD). Furthermore, BFT contrasted HG-induced decreases in pSTAT3 (supplemental Figure IXE), pAkt and Akt activity (supplemental Figure IXF and IXG) and peNOS and pFOXO-1 (supplemental Figure IXH and IXI). Of note, HG reduced the nuclear localization of Akt, which is necessary for Akt to induce Pim-1 expression and phosphorylate or inhibit FOXOs,34 but BFT restored proper nuclear Akt levels (supplemental Figure IXJ).

Infection of cardiomyocytes with *Ad.DN-Akt*, verified by assessing the expression of hemagglutinin tag (data not shown), abrogated the stimulating action of BFT on pAkt without affecting STAT3. Furthermore, *Ad.DN-Akt* significantly inhibited the antiapoptotic action of BFT under HG and contrasted the effects of BFT on Pim-1, pBad, and Bcl-2 (supplemental Figure XA through XF). Prevention of apoptosis by BFT was similarly

reduced by the PI3K inhibitor LY294002 (supplemental Figure XG). Treatment of cardiomyocytes with STAT3 inhibitor reduced basal and BFT-stimulated pSTAT3 levels without affecting pAkt (supplemental Figure XH and XI). STAT3 inhibition potentiated Pim-1 downregulation and cardiomyocyte apoptosis under HG (supplemental Figure XJ and XM). It also contrasted BFT in preserving Pim-1 expression and to a lesser extent pBad and Bcl-2 (supplemental Figure XJ through XL) but was ineffective in inhibiting the antiapoptotic action of BFT, suggesting that pAkt induction by BFT could compensate for STAT3/Pim-1 deficit to support cardiomyocyte viability under HG conditions.

## Discussion

In a previous report in streptozotocin mice, a 2-week administration of BFT preserved in vitro contractile properties and intracellular $Ca^{2+}$ kinetics of cardiomyocytes.35 To the best of our knowledge, however, this is the first study to show the therapeutic potential of long-term treatment with BFT for prevention of cardiomyopathy in models of types 1 and 2 DM, which is particularly relevant in light of the prevalent incidence of cardiomyopathy in patients with type 2 DM. The effect of BFT was documented by echocardiography follow-up of LV function, Millar transducer measurement of LV pressure, and cardiac morphometry. Furthermore, we newly reported that BFT prevents myocardial microvascular rarefaction, thereby improving myocardial perfusion of diabetic hearts. The role of microcirculation in the pathogenesis of diabetic cardiomyopathy has been highlighted by a study in which gene therapy with vascular endothelial growth factor-A prevented capillary rarefaction and cardiac dysfunction in mice.36 Our in vitro studies, however, indicate a direct action of BFT on cardiomyocyte survival; thus, the improved myocardial blood flow might additively contribute to preservation of cell viability and cardiac performance.

Another novel contribution of this study is the first documentation of chronologic alterations in components of prosurvival signaling during progression of cardiomyopathy and of the impact of BFT on these molecular changes. Our results of reduced myocardial pAkt levels in failing diabetic hearts are consistent with earlier reports in mice with long-standing DM,37,38 yet the mechanism responsible for Akt inhibition was not clear. Emerging evidence indicates that HG-induced activation of hexosamine pathway plays a role in the etiology of diabetic cardiomyopathy through O-GlcNAc modification of transcription factors and proteins involved in cardiomyocyte function.39 We show for the first time the combination of reduced Akt activity and increased O-GlcNAc modification of Akt in myocardium of diabetic mice. Inactivation of Akt may account for increased cardiomyocyte apoptosis in failing diabetic hearts because Akt directly controls the phosphorylation and sequestration of the Bad and FOXO transcription factors.40 Of note, BFT, which reportedly reduces the glucose flux to the hexosamine pathway,17 abrogated DM-induced O-GlcNAc modification of Akt, thereby restoring Akt activity and Bad and FOXO-1 phosphorylation levels.

One intriguing aspect of our results consists of increased Akt activity at early stages of cardiomyopathy in type 1 diabetic mice, which is possibly a compensatory attempt to combat DM-induced damage. On the other hand, chronic Akt activation could have detrimental effects on the heart through inhibition of insulin receptor substrate/PI3K signaling and disruption of the coordinated association between adaptive cardiac hypertrophy and microvascular growth.41,42 Of note, while confirming the reduction of microvascular density in failing diabetic hearts, our data show no evidence of hypertrophic remodeling during initial increase of Akt in type 1 diabetic hearts. The time duration of Akt activation might have been too short to sustain LV hypertrophy in our experimental setting. Furthermore, the dual action of Akt on cardiomyocyte survival and growth could depend on the specific intracellular location of activated Akt.10

Many of the cardiac actions of Akt are ascribed to be Pim-1 dependent. For instance, Akt activation induces Pim-1 expression, but forced expression of Akt failed to protect the infarcted myocardium of Pim-1-deficient mice.11 Pim-1-induced cardioprotection is reportedly mediated by upregulation of Bcl-2 and Bcl-XL as well as phosphorylation and inactivation of Bad. Our in vitro findings showing that PI3K/Akt inhibition abrogates the action of BFT on cardiomyocyte survival under HG and contrasts the stimulatory effect of BFT on Pim-1 and Bcl-2 indicate that Akt is a crucial facet of cardioprotection exerted by this compound. This concept is reinforced by the finding that BFT-induced Akt upregulation in HG-challenged cardiomyocytes is sufficient for the prevention of apoptosis under STAT3 inhibition.

Our in vivo findings in type 1 diabetic mice showed, however, a situation more intricate than predicted in vitro. In the compensated phase, changes in myocardial pAkt and Pim-1 levels were not synchronous, with Pim-1 starting to decrease earlier than pAkt. This pattern might suggest a crucial role of Pim-1 in early diastolic dysfunction and indicate the contribution of mechanisms independent of Akt in Pim-1 downregulation. One possible candidate is STAT3, which upregulates Pim-1 expression by binding with its promoter.43 In line, we found that pSTAT3 is reduced at compensated stages of diabetic cardiomyopathy. In addition, DM induced the expression of PP2A, which is known to dephosphorylate and inactivate Pim-1.30 An additional explanation for the apparent discrepancy between high pAkt and low Pim-1 levels at the early stage of cardiomyopathy is that pAkt might remain sequestered in the cytosol and thus unable to upregulate Pim-1 expression. This is in line with the reduced nuclear localization of Akt in HG-challenged cardiomyocytes. Of note, BFT prevented the reduction in pSTAT3 and preserved nuclear Akt but failed to decrease PP2A. Thus, the action of BFT seemingly affects positive regulators of Pim-1 rather than mechanisms of Pim-1 destabilization.

The protective action of BFT extends to other mechanisms implicated in the pathogenesis of diabetic cardiomyopathy. Hyperglycemia causes oxidative stress by inducing reactive oxygen species and dampening antioxidant generation. In this study, we newly showed that BFT reduces superoxide and hydroxyl radical levels in diabetic hearts by inducing the activation of pentose phosphate pathway, which regenerates the antioxidant NADPH. Furthermore, superoxide overproduction by hyperglycemia inhibits the glycolytic enzyme GAPDH,17 thereby diverting metabolites from glycolysis into major pathways of hyperglycemic damage.20 Importantly, we showed that these effects of DM were inhibited by BFT as evidenced by increased GAPDH activity and reduced AGE levels. Prevention of AGE accumulation could account for inhibition of interstitial fibrosis by BFT.

In conclusion, our results illustrate fundamental mechanisms that are involved in the pathogenesis of diabetic cardiomyopathy and could be prevented by BFT (summarized in supplemental Figure XI). Implications of the present preclinical study to the clinical field should be evaluated cautiously in the light of similarities and differences of cardiomyopathy developing in patients with diabetes and diabetic animal models. Furthermore, the dosage and time schedule of BFT supplementation represent a crucial issue, as for other preventive treatments, that sustained activation of proto-oncogenes, such as Akt and Pim-1, might increase the risk of cancer. This concern, however, is not supported by our results showing no evidence of adverse effects but. Rather. improved survival of diabetic mice treated with a high dose of BFT.

## CLINICAL PERSPECTIVE

Diabetes mellitus is a potent and prevalent risk factor for heart failure, independently of coronary artery disease or hypertension. Importantly, diabetes mellitus can affect cardiac

structure and function independently of coexisting hypertension or ischemic heart disease, resulting in a condition named diabetic cardiomyopathy. Diabetic cardiomyopathy has an insidious onset, manifesting with isolated diastolic dysfunction, which progresses with time to global heart failure. The present study unravels distinct molecular signatures of the progression of diabetic cardiomyopathy from early and probably reversible stages to more advanced heart remodeling and dilatation. In particular, we clarified a possible link between the metabolic disorder and epigenetic changes that make the prosurvival Akt/Pim1 duo dysfunctional, thereby compromising the heart's performance. This discovery opens new windows of therapeutic opportunity to combat this increasingly harmful complication of diabetes. Importantly, vitamin B1 analogue benfotiamine is able to beneficially interfere with the Akt/Pim1 disturbed signaling and thus prevents the mismatch between angiogenesis and cardiomyocyte remodeling in the diabetic heart. Whether benfotiamine is therapeutically useful needs now to be demonstrated by clinical trials. Furthermore, because the main action of benfotiamine is to boost the activity of transketolase, a key enzyme of the pentose phosphate pathway, and because transketolase activity is reduced in diabetes, it is important to determine whether patients with reduced transketolase activity are susceptible to develop an accelerated form of cardiomyopathy. If this is proved true, patients with low transketolase would become the best candidates to benfotiamine treatment.

## Supplementary Material

Refer to Web version on PubMed Central for supplementary material.

## Acknowledgments

We thank Nicolle Kraenkel for her assistance in quantitative reverse transcription polymerase chain reaction and Paul Salvage for his assistance in immunohistochemistry.

Sources of Funding

This study was supported by a project grant from Diabetes UK (RD06/0003413) and Resolve (202047). Dr Emanueli holds a British Heart Foundation Basic Science fellowship (BS/05/01), and at the time of this study, Dr Caporali was a British Heart Foundation doctoral student (FS/05/113/19965).

## References

1. Boudina S, Abel ED. Diabetic cardiomyopathy revisited. Circulation. 2007; 115:3213–3223. [PubMed: 17592090]
2. Boyer JK, Thanigaraj S, Schechtman KB, Perez JE. Prevalence of ventricular diastolic dysfunction in asymptomatic, normotensive patients with diabetes mellitus. Am J Cardiol. 2004; 93:870–875. [PubMed: 15050491]
3. Liu JE, Robbins DC, Palmieri V, Bella JN, Roman MJ, Fabsitz R, Howard BV, Welty TK, Lee ET, Devereux RB. Association of albuminuria with systolic and diastolic left ventricular dysfunction in type 2 diabetes: the Strong Heart Study. J Am Coll Cardiol. 2003; 41:2022–2028. [PubMed: 12798576]
4. Arnold JM, Yusuf S, Young J, Mathew J, Johnstone D, Avezum A, Lonn E, Pogue J, Bosch J. Prevention of heart failure in patients in the Heart Outcomes Prevention Evaluation (HOPE) study. Circulation. 2003; 107:1284–1290. [PubMed: 12628949]
5. Elkeles RS, Godsland IF, Feher MD, Rubens MB, Roughton M, Nugara F, Humphries SE, Richmond W, Flather MD. Coronary calcium measurement improves prediction of cardiovascular events in asymptomatic patients with type 2 diabetes: the PREDICT study. Eur Heart J. 2008; 29:2244–2251. [PubMed: 18573867]

6. Rodrigues B, Cam MC, McNeill JH. Metabolic disturbances in diabetic cardiomyopathy. Mol Cell Biochem. 1998; 180:53–57. [PubMed: 9546630]
7. Bauters C, Lamblin N, McFadden EP, Van Belle E, Millaire A, de Groote P. Influence of diabetes mellitus on heart failure risk and outcome. Cardiovasc Diabetol. 2003; 2:1. [PubMed: 12556246]
8. Clark RJ, McDonough PM, Swanson E, Trost SU, Suzuki M, Fukuda M, Dillmann WH. Diabetes and the accompanying hyperglycemia impairs cardiomyocyte calcium cycling through increased nuclear O-GlcNAcylation. J Biol Chem. 2003; 278:44230–44237. [PubMed: 12941958]
9. Kajstura J, Fiordaliso F, Andreoli AM, Li B, Chimenti S, Medow MS, Limana F, Nadal-Ginard B, Leri A, Anversa P. IGF-1 overexpression inhibits the development of diabetic cardiomyopathy and angiotensin II-mediated oxidative stress. Diabetes. 2001; 50:1414–1424. [PubMed: 11375343]
10. Catalucci D, Condorelli G. Effects of Akt on cardiac myocytes: location counts. Circ Res. 2006; 99:339–341. [PubMed: 16917099]
11. Muraski JA, Rota M, Misao Y, Fransioli J, Cottage C, Gude N, Esposito G, Delucchi F, Arcarese M, Alvarez R, Siddiqi S, Emmanuel GN, Wu W, Fischer K, Martindale JJ, Glembotski CC, Leri A, Kajstura J, Magnuson N, Berns A, Beretta RM, Houser SR, Schaefer EM, Anversa P, Sussman MA. Pim-1 regulates cardiomyocyte survival downstream of Akt. Nat Med. 2007; 13:1467–1475. [PubMed: 18037896]
12. Amaravadi R, Thompson CB. The survival kinases Akt and Pim as potential pharmacological targets. J Clin Invest. 2005; 115:2618–2624. [PubMed: 16200194]
13. Westermann D, Van Linthout S, Dhayat S, Dhayat N, Escher F, Bucker-Gartner C, Spillmann F, Noutsias M, Riad A, Schultheiss HP, Tschope C. Cardioprotective and anti-inflammatory effects of interleukin converting enzyme inhibition in experimental diabetic cardiomyopathy. Diabetes. 2007; 56:1834–1841. [PubMed: 17473225]
14. Hilfiker-Kleiner D, Hilfiker A, Fuchs M, Kaminski K, Schaefer A, Schieffer B, Hillmer A, Schmiedl A, Ding Z, Podewski E, Podewski E, Poli V, Schneider MD, Schulz R, Park JK, Wollert KC, Drexler H. Signal transducer and activator of transcription 3 is required for myocardial capillary growth, control of interstitial matrix deposition, and heart protection from ischemic injury. Circ Res. 2004; 95:187–195. [PubMed: 15192020]
15. Jermendy G. Evaluating thiamine deficiency in patients with diabetes. Diab Vasc Dis Res. 2006; 3:120–121. [PubMed: 17058632]
16. Xu Y, Osborne BW, Stanton RC. Diabetes causes inhibition of glucose-6-phosphate dehydrogenase via activation of PKA, which contributes to oxidative stress in rat kidney cortex. Am J Physiol Renal Physiol. 2005; 289:F1040–F1047. [PubMed: 15956780]
17. Du XL, Edelstein D, Rossetti L, Fantus IG, Goldberg H, Ziyadeh F, Wu J, Brownlee M. Hyperglycemia-induced mitochondrial superoxide overproduction activates the hexosamine pathway and induces plasminogen activator inhibitor-1 expression by increasing Sp1 glycosylation. Proc Natl Acad Sci U S A. 2000; 97:12222–12226. [PubMed: 11050244]
18. Du X, Matsumura T, Edelstein D, Rossetti L, Zsengeller Z, Szabo C, Brownlee M. Inhibition of GAPDH activity by poly(ADP-ribose) polymerase activates three major pathways of hyperglycemic damage in endothelial cells. J Clin Invest. 2003; 112:1049–1057. [PubMed: 14523042]
19. Gadau S, Emanueli C, Van Linthout S, Graiani G, Todaro M, Meloni M, Campesi I, Invernici G, Spillmann F, Ward K, Madeddu P. Benfotiamine accelerates the healing of ischaemic diabetic limbs in mice through protein kinase B/Akt-mediated potentiation of angiogenesis and inhibition of apoptosis. Diabetologia. 2006; 49:405–420. [PubMed: 16416271]
20. Hammes HP, Du X, Edelstein D, Taguchi T, Matsumura T, Ju Q, Lin J, Bierhaus A, Nawroth P, Hannak D, Neumaier M, Bergfeld R, Giardino I, Brownlee M. Benfotiamine blocks three major pathways of hyperglycemic damage and prevents experimental diabetic retinopathy. Nat Med. 2003; 9:294–299. [PubMed: 12592403]
21. Thornalley PJ, Jahan I, Ng R. Suppression of the accumulation of triose-phosphates and increased formation of methylglyoxal in human red blood cells during hyperglycaemia by thiamine in vitro. J Biochem. 2001; 129:543–549. [PubMed: 11275553]

22. Fujii EY, Nakayama M, Nakagawa A. Concentrations of receptor for advanced glycation end products, VEGF and CML in plasma, follicular fluid, and peritoneal fluid in women with and without endometriosis. Reprod Sci. 2008; 15:1066–1074. [PubMed: 19088375]
23. de Simone G, Wallerson DC, Volpe M, Devereux RB. Echocardiographic measurement of left ventricular mass and volume in normotensive and hypertensive rats. Necropsy validation. Am J Hypertens. 1990; 3:688–696. [PubMed: 2222977]
24. Smith RS, Gao L, Chao L, Chao J. Tissue kallikrein and kinin infusion promotes neovascularization in limb ischemia. Biol Chem. 2008; 389:725–730. [PubMed: 18627294]
25. Caporali A, Sala-Newby GB, Meloni M, Graiani G, Pani E, Cristofaro B, Newby AC, Madeddu P, Emanueli C. Identification of the prosurvival activity of nerve growth factor on cardiac myocytes. Cell Death Differ. 2008; 15:299–311. [PubMed: 17992191]
26. Catalano RD, Johnson MH, Campbell EA, Charnock-Jones DS, Smith SK, Sharkey AM. Inhibition of Stat3 activation in the endometrium prevents implantation: a nonsteroidal approach to contraception. Proc Natl Acad Sci U S A. 2005; 102:8585–8590. [PubMed: 15937114]
27. Yang X, Ongusaha PP, Miles PD, Havstad JC, Zhang F, So WV, Kudlow JE, Michell RH, Olefsky JM, Field SJ, Evans RM. Phosphoinositide signalling links O-GlcNAc transferase to insulin resistance. Nature. 2008; 451:964–969. [PubMed: 18288188]
28. Vosseller K, Wells L, Lane MD, Hart GW. Elevated nucleocytoplasmic glycosylation by O-GlcNAc results in insulin resistance associated with defects in Akt activation in 3T3-L1 adipocytes. Proc Natl Acad Sci USA. 2002; 99:5313–5318. [PubMed: 11959983]
29. Hirano T, Ishihara K, Hibi M. Roles of STAT3 in mediating the cell growth, differentiation and survival signals relayed through the IL-6 family of cytokine receptors. Oncogene. 2000; 19:2548–2556. [PubMed: 10851053]
30. Ma J, Arnold HK, Lilly MB, Sears RC, Kraft AS. Negative regulation of Pim-1 protein kinase levels by the B56beta subunit of PP2A. Oncogene. 2007; 26:5145–5153. [PubMed: 17297438]
31. Luo B, Soesanto Y, McClain DA. Protein modification by O-linked GlcNAc reduces angiogenesis by inhibiting Akt activity in endothelial cells. Arterioscler Thromb Vasc Biol. 2008; 28:651–657. [PubMed: 18174452]
32. Datta SR, Dudek H, Tao X, Masters S, Fu H, Gotoh Y, Greenberg ME. Akt phosphorylation of BAD couples survival signals to the cell-intrinsic death machinery. Cell. 1997; 91:231–241. [PubMed: 9346240]
33. Aho TL, Sandholm J, Peltola KJ, Mankonen HP, Lilly M, Koskinen PJ. Pim-1 kinase promotes inactivation of the pro-apoptotic Bad protein by phosphorylating it on the Ser112 gatekeeper site. FEBS Lett. 2004; 571:43–49. [PubMed: 15280015]
34. Miyamoto S, Rubio M, Sussman MA. Nuclear and mitochondrial signalling Akts in cardiomyocytes. Cardiovasc Res. 2009; 82:272–285. [PubMed: 19279164]
35. Ceylan-Isik AF, Wu S, Li Q, Li SY, Ren J. High-dose benfotiamine rescues cardiomyocyte contractile dysfunction in streptozotocin-induced diabetes mellitus. J Appl Physiol. 2006; 100:150–156. [PubMed: 16166234]
36. Yoon YS, Uchida S, Masuo O, Cejna M, Park JS, Gwon HC, Kirchmair R, Bahlman F, Walter D, Curry C, Hanley A, Isner JM, Losordo DW. Progressive attenuation of myocardial vascular endothelial growth factor expression is a seminal event in diabetic cardiomyopathy: restoration of microvascular homeostasis and recovery of cardiac function in diabetic cardiomyopathy after replenishment of local vascular endothelial growth factor. Circulation. 2005; 111:2073–2085. [PubMed: 15851615]
37. Huisamen B. Protein kinase B in the diabetic heart. Mol Cell Biochem. 2003; 249:31–38. [PubMed: 12956395]
38. Ren J, Duan J, Thomas DP, Yang X, Sreejayan N, Sowers JR, Leri A, Kajstura J, Gao F, Anversa P. IGF-I alleviates diabetes-induced RhoA activation, eNOS uncoupling, and myocardial dysfunction. Am J Physiol Regul Integr Comp Physiol. 2008; 294:R793–R802. [PubMed: 18199585]
39. Hart GW, Housley MP, Slawson C. Cycling of O-linked beta-*N*-acetylglucosamine on nucleocytoplasmic proteins. Nature. 2007; 446:1017–1022. [PubMed: 17460662]

40. Walsh K. Akt signaling and growth of the heart. Circulation. 2006; 113:2032–2034. [PubMed: 16651482]
41. Nagoshi T, Matsui T, Aoyama T, Leri A, Anversa P, Li L, Ogawa W, del Monte F, Gwathmey JK, Grazette L, Hemmings BA, Kass DA, Champion HC, Rosenzweig A. PI3K rescues the detrimental effects of chronic Akt activation in the heart during ischemia/reperfusion injury. J Clin Invest. 2005; 115:2128–2138. [PubMed: 16007268]
42. Shiojima I, Sato K, Izumiya Y, Schiekofer S, Ito M, Liao R, Colucci WS, Walsh K. Disruption of coordinated cardiac hypertrophy and angio-genesis contributes to the transition to heart failure. J Clin Invest. 2005; 115:2108–2118. [PubMed: 16075055]
43. Bachmann M, Moroy T. The serine/threonine kinase Pim-1. Int J Biochem Cell Biol. 2005; 37:726–730. [PubMed: 15694833]


Europe PMC Funders Author Manuscripts

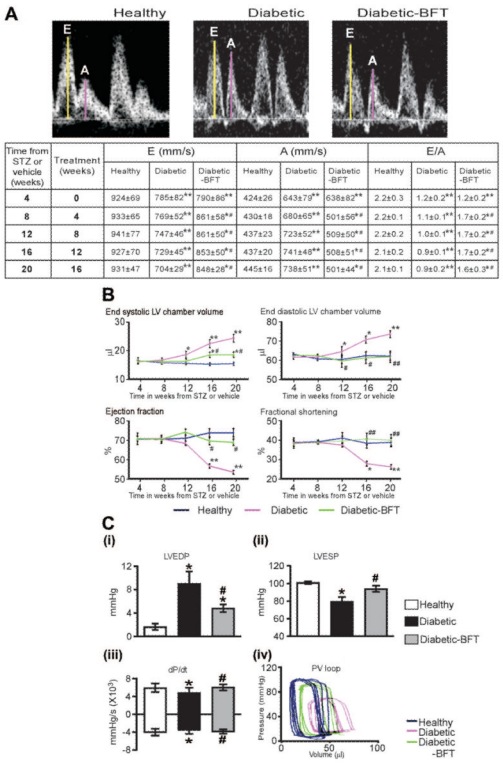


| Time from STZ or vehicle (weeks) | Treatment (weeks) | E (mm/s) | | | A (mm/s) | | | E/A | | |
|---|---|---|---|---|---|---|---|---|---|---|
| | | Healthy | Diabetic | Diabetic -BFT | Healthy | Diabetic | Diabetic -BFT | Healthy | Diabetic | Diabetic -BFT |
| 4 | 0 | 924±69 | 785±82** | 790±86** | 424±26 | 643±79** | 638±82** | 2.2±0.3 | 1.2±0.2** | 1.2±0.2** |
| 8 | 4 | 933±65 | 769±52** | 861±58*# | 430±18 | 680±65** | 501±56*# | 2.2±0.1 | 1.1±0.1** | 1.7±0.2*# |
| 12 | 8 | 941±77 | 747±46** | 861±50*# | 437±23 | 723±52** | 509±50*# | 2.2±0.2 | 1.0±0.1** | 1.7±0.2*# |
| 16 | 12 | 927±70 | 729±45** | 853±50*# | 437±20 | 741±48** | 508±51*# | 2.1±0.2 | 0.9±0.1** | 1.7±0.2*# |
| 20 | 16 | 931±47 | 704±29** | 846±26*# | 445±16 | 738±51** | 501±44*# | 2.1±0.1 | 0.9±0.2** | 1.6±0.3*# |

**Figure 1.**

BFT prevents ventricular dysfunction in type 1 DM. A, Representative pulsed Doppler images and table showing the effect of BFT on E/A ratio. E and A waves represent mitral valve velocity during early diastolic filling and atrial contraction, respectively (n=16 mice per group). B, Indexes of LV function assessed by echocardiography (n=16 per group). C (i–iii), Bar graphs showing the effect of BFT on LV end-diastolic pressure (LVEDP), LV end-systolic pressure (LVESP), and maximum and minimum rates of developed pressure (dP/dt) at 16 weeks of treatment (n=12 per group). C (iv), Representative pressure-volume (PV) loops obtained by integrated measurement of LV pressure (Millar catheter) and volume (echocardiography). Values are mean±SD. BFT did not affect cardiac function in healthy mice (data not shown). STZ indicates streptozotocin. Results of pairwise comparison are as follows: **P*<0.01 and ***P*<0.01 versus healthy controls; #*P*<0.01 and ##*P*<0.01 versus vehicle-treated diabetic mice.




Europe PMC Funders Author Manuscripts

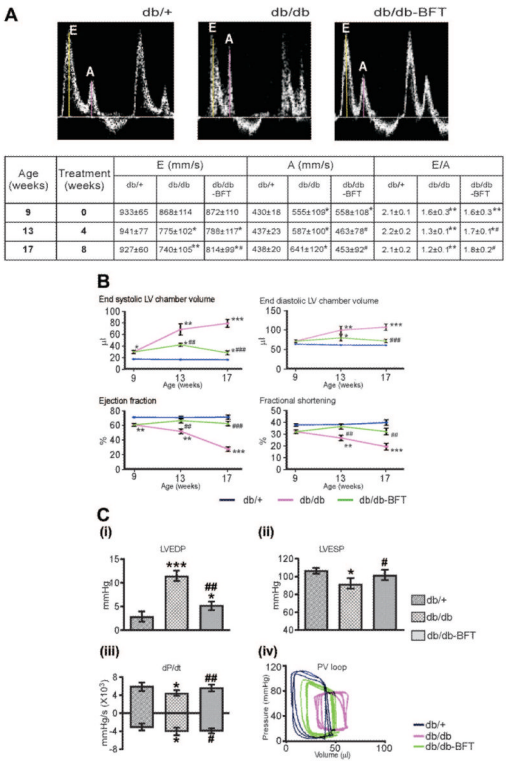


| Age (weeks) | Treatment (weeks) | E (mm/s) | | | A (mm/s) | | | E/A | | |
|---|---|---|---|---|---|---|---|---|---|---|
| | | db/+ | db/db | db/db -BFT | db/+ | db/db | db/db -BFT | db/+ | db/db | db/db -BFT |
| 9 | 0 | 933±65 | 868±114 | 872±110 | 430±18 | 555±109* | 558±108* | 2.1±0.1 | 1.6±0.3** | 1.6±0.3** |
| 13 | 4 | 941±77 | 775±102* | 788±117* | 437±23 | 587±100* | 463±78# | 2.2±0.2 | 1.3±0.1** | 1.7±0.1## |
| 17 | 8 | 927±60 | 740±105** | 814±99** | 438±20 | 641±120* | 453±92# | 2.1±0.2 | 1.2±0.1** | 1.8±0.2# |

**Figure 2.**

BFT prevents ventricular dysfunction in type 2 DM. A, Representative images and table showing the effect of BFT on Doppler E/A ratio (n=10 per group). B, Echocardiography indices of LV function (n=10 per group). C (i–iii), Bar graphs showing the effect of BFT on LV pressure and volume indices at 8 weeks of treatment (n=10 per group). C (iv), Representative pressure-volume loops. Values are mean±SD. BFT did not affect cardiac function in db/+ mice (data not shown). LVEDP indicates LV end-diastolic pressure; LVESP, LV end-systolic pressure; dP/dt, maximum and minimum rates of developed pressure; and PV, pressure-volume. Results of pairwise comparison are as follows: **P*<0.01, ***P*<0.001, and ****P*<0.0001 versus db/+ mice; #*P*<0.01, ##*P*<0.001, and ###*P*<0.0001 versus vehicle-treated db/db mice.




Europe PMC Funders Author Manuscripts

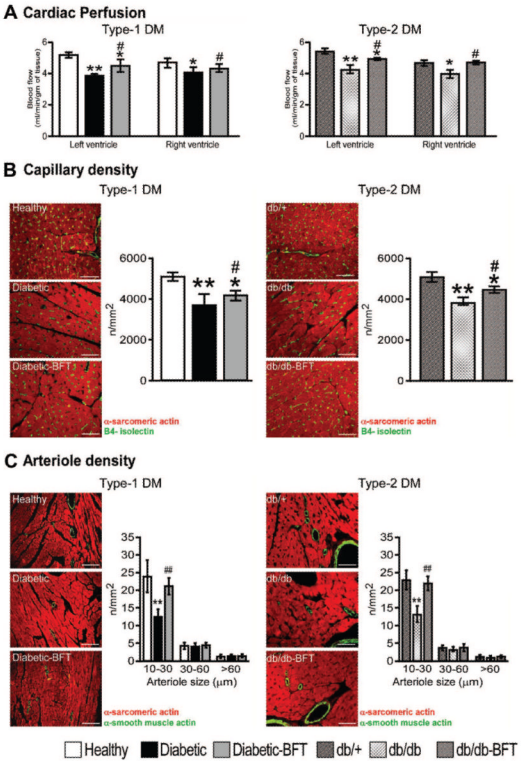


**Figure 3.**

BFT improves myocardial blood flow and vascularization. A, Bar graphs showing the effect of BFT on myocardial blood flow in type 1 (n=6 per group, 16-week treatment) and type 2 diabetic mice (n=4 per group, 8-week treatment). Age-matched untreated healthy controls for the 2 diabetic groups are shown for comparison (n=4 to 6 mice). B, Representative immunohistochemistry images of microvasculature and bar graphs showing LV capillary density of diabetic mice (n=6, treatment duration as above). C, Representative immunohistochemistry images of microvasculature and bar graphs showing LV arteriole density of diabetic mice (n=6 per group, treatment duration as above). Age-matched untreated healthy controls for type 1 DM and db/+ for type 2 DM groups are shown for comparison (n=6). Scale bars are 50 $\mu$m. Results of pairwise comparison are as follows: *$P$<0.01 and **$P$<0.001 versus healthy controls in type 1 DM or db/+ mice in type 2 DM; #$P$<0.01 and ##$P$<0.001 versus vehicle-treated diabetic mice in type 1 DM or db/db mice in type 2 DM.




Europe PMC Funders Author Manuscripts

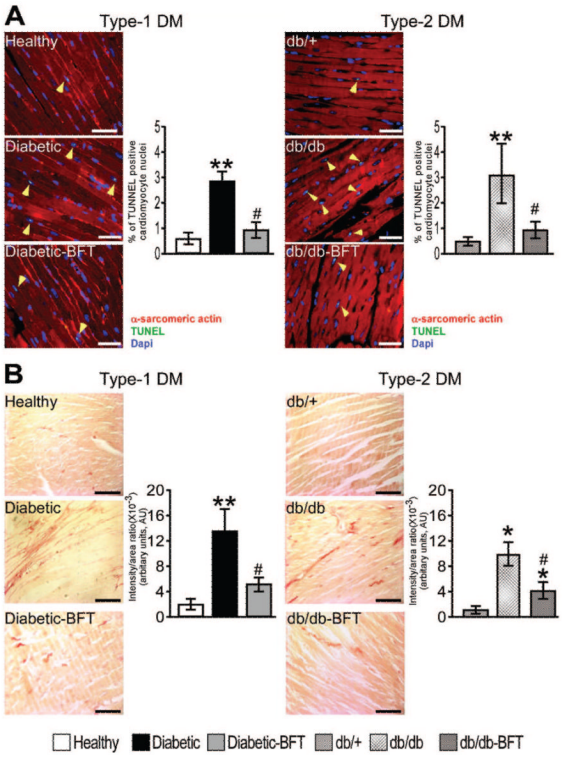


**Figure 4.**

BFT prevents cardiomyocyte apoptosis and cardiac fibrosis. A and B, Representative microphotographs and bar graphs showing the effect of BFT on cardiomyocyte apoptosis and interstitial fibrosis (n=5 per group). Scale bars are 50 $\mu$m. Treatment duration and statistical analysis as in Figure 3. *$P$<0.01 and **$P$<0.001 versus healthy controls in type 1 DM or db/+ mice in type 2 DM; #$P$<0.01 versus vehicle-treated diabetic mice in type 1 DM or db/db mice in type 2 DM.




Europe PMC Funders Author Manuscripts

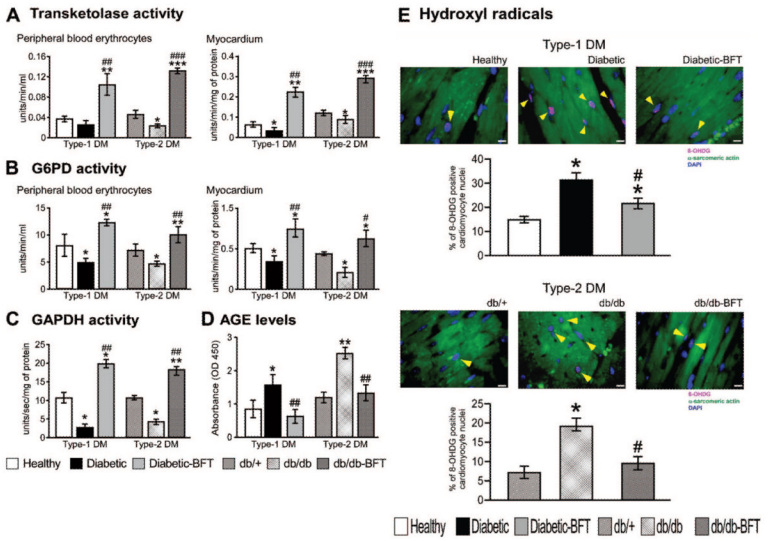


**Figure 5.**

BFT activates the pentose phosphate pathway and inhibits reactive oxygen species. Bar graphs showing the effect of BFT on transketolase (A), glucose-6-phosphate dehydrogenase (G6PD) (B), GADPH (C), and AGE (D) (n=5 per group, each assay in triplicate). Representative microphotographs and bar graphs showing myocardial hydroxyl radical levels (E) (n=5 per group). Treatment duration and statistical analysis as in Figure 3. 8-OHDG indicates 8-hydroxydeoxyguanosine. **P*<0.01, ***P*<0.001, and ****P*<0.0001 versus healthy controls in type 1 DM or db/+ mice in type 2 DM; #*P*<0.001, ##*P*<0.001, and ###*P*<0.01 versus vehicle-treated diabetic mice in type 1 DM or db/db mice in type 2 DM.




Europe PMC Funders Author Manuscripts

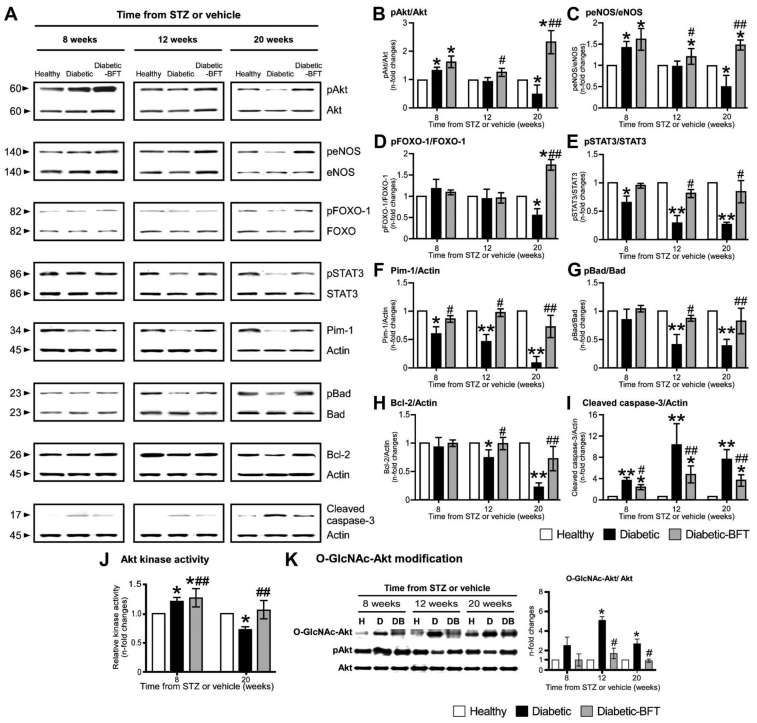


**Figure 6.**

BFT stimulates prosurvival signaling in type 1 DM. Representative blots (A) and bar graphs (B through I) showing the levels of pAkt, peNOS, pFOXO-1, pSTAT3, Pim-1, pBad, Bcl-2, and cleaved caspase-3 (n=4 per group). Bar graphs showing myocardial Akt activity (J). Representative immunoblots and bar graphs showing O-GlcNAc modification of Akt in diabetic hearts (K) (n=4 per group). Values are expressed as n-fold changes toward age-matched healthy controls. STZ indicates streptozotocin. Siegel-Tukey test detected statistical differences as follows: **P*<0.01 and ***P*<0.001 versus healthy controls; #*P*<0.01 and ##*P*<0.001 versus vehicle-treated diabetic mice.




Europe PMC Funders Author Manuscripts

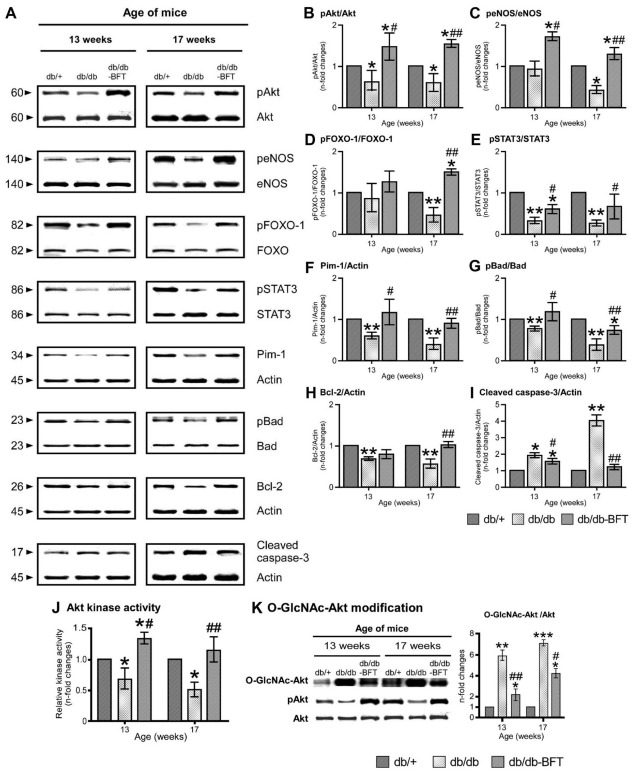


**Figure 7.**

BFT stimulates prosurvival signaling in type 2 DM. Representative blots (A) and bar graphs (B through I) showing the levels of pAkt, peNOS, pFOXO-1, pSTAT3, Pim-1, pBad, Bcl-2, and cleaved caspase-3 (n=4 per group). Bar graphs showing myocardial Akt activity (J). Representative immunoblots and bar graphs showing O-GlcNAc modification of Akt in diabetic hearts (K) (n=4 per group). Values are expressed as n-fold changes toward age-matched healthy controls. Siegel-Tukey test detected statistical differences are as follows: **P*<0.01, ***P*<0.001, and ****P*<0.001 versus db/+ mice; #*P*<0.01 and ##*P*<0.001 versus vehicle-treated db/db mice.




Europe PMC Funders Author Manuscripts